

## Activation of Gold on Titania: Adsorption and Reaction of SO<sub>2</sub> on Au/TiO<sub>2</sub>(110)

José A. Rodríguez,<sup>\*,†</sup> Gang Liu,<sup>†</sup> Tomas Jirsak,<sup>†</sup> Jan Hrbek,<sup>†</sup> Zhipeng Chang,<sup>†</sup> Joseph Dvorak,<sup>†</sup> and Amitesh Maiti<sup>‡</sup>

Contribution from the Department of Chemistry, Brookhaven National Laboratory, Upton, New York 11973, and Accelrys Inc, 9685 Scranton Road, San Diego, California 92121

Received January 23, 2002

**Abstract:** Synchrotron-based high-resolution photoemission and first-principles density-functional slab calculations were used to study the interaction of gold with titania and the chemistry of SO<sub>2</sub> on Au/TiO<sub>2</sub>(110) surfaces. The deposition of Au nanoparticles on TiO<sub>2</sub>(110) produces a system with an extraordinary ability to adsorb and dissociate SO<sub>2</sub>. In this respect, Au/TiO<sub>2</sub> is much more chemically active than metallic gold or stoichiometric titania. On Au(111) and rough polycrystalline surfaces of gold, SO<sub>2</sub> bonds weakly and desorbs intact at temperatures below 200 K. For the adsorption of SO<sub>2</sub> on TiO<sub>2</sub>(110) at 300 K, SO<sub>4</sub> is the only product (SO<sub>2</sub> + O<sub>oxide</sub> → SO<sub>4,ads</sub>). In contrast, Au/TiO<sub>2</sub>(110) surfaces ( $\theta_{\text{Au}} \leq 0.5$  ML) fully dissociate the SO<sub>2</sub> molecule under identical reaction conditions. Interactions with titania electronically perturb gold, making it more chemically active. Furthermore, our experimental and theoretical results show quite clearly that not only gold is perturbed when gold and titania interact. *The adsorbed gold, on its part, enhances the reactivity of titania by facilitating the migration of O vacancies from the bulk to the surface of the oxide.* In general, the complex coupling of these phenomena must be taken into consideration when trying to explain the unusual chemical and catalytic activity of Au/TiO<sub>2</sub>. In many situations, the oxide support can be much more than a simple spectator.

### I. Introduction

Bulk metallic gold typically exhibits a very low chemical and catalytic activity.<sup>1,2</sup> Among the transition metals, gold is by far the least reactive and is often referred to as the “coinage metal”. The low reactivity of metallic Au is a consequence of combining a deep-lying valence d band and very diffuse valence s,p orbitals.<sup>2,3</sup> Recently, gold has become the subject of a lot of attention due to its unusual catalytic properties when dispersed on some oxide supports (TiO<sub>2</sub>, CrO<sub>x</sub>, MnO<sub>x</sub>, Fe<sub>2</sub>O<sub>3</sub>, Al<sub>2</sub>O<sub>3</sub>, MgO).<sup>4–19</sup> The Au/TiO<sub>2</sub> system is particularly interesting.<sup>5,11–17</sup>

Gold particles supported on titania are active catalysts for the low-temperature oxidation of CO, the selective oxidation of propene, and photocatalytic oxidations used for environmental cleanup.<sup>5–7,14</sup> Several models have been proposed for explaining the activation of supported gold:<sup>5,7,9,10,18</sup> from special electronic properties resulting from the limited size of the active gold particles (usually less than 10 nm),<sup>5,7,15a,19</sup> to the effects of metal–support interactions (i.e. charge transfer between the oxide and gold).<sup>7,10,12,18</sup> In principle, the active sites for the catalytic reactions could be located only on the supported Au particles or on the perimeter of the gold–oxide interface.<sup>5,7,9b,15b</sup> The Au/TiO<sub>2</sub>(110) surface appears as an ideal and well-defined system to examine some of these hypotheses in a controlled manner.<sup>7,9,11–13,20</sup>

\* Corresponding author. FAX: 631-344-5815. E-mail: rodriguez@bnl.gov.

<sup>†</sup> Brookhaven National Laboratory.

<sup>‡</sup> Accelrys Inc.

- (1) (a) Thomas, J. M.; Thomas, W. J. *Principles and Practice of Heterogeneous Catalysis*; VCH: New York, 1997. (b) Somorjai, G. A. *Introduction to Surface Chemistry and Catalysis*; Wiley: New York, 1994.
- (2) (a) Cotton, F. A.; Wilkinson, G. *Advanced Inorganic Chemistry*, 5th ed; Wiley: New York, 1988. (b) Huheey, J. E. *Inorganic Chemistry*, 3rd ed; Harper & Row: New York, 1983. (c) Bond, G. C.; Thompson, D. T. *Catal. Rev. Sci. Eng.* **1999**, *41*, 319.
- (3) (a) Hammer, B.; Nørskov, J. K. *Nature* **1995**, *376*, 238. (b) Hammer, B.; Nørskov, J. K. *Adv. Catal.* **2000**, *45*, 71. (c) Shustorovich, E.; Baetzold, R. C. *Science* **1985**, *227*, 876. (d) Rodriguez, J. A.; Kuhn, M. *Surf. Sci.* **1995**, *330*, L657.
- (4) Haruta, M.; Tsubota, S.; Kobayashi, T.; Kageyama, H.; Genet, M. J.; Delmont, B. *J. Catal.* **1993**, *144*, 175.
- (5) Haruta, M. *Catal. Today* **1997**, *36*, 153.
- (6) (a) Lin, S. D.; Bollinger, M.; Vannice, M. A. *Catal. Lett.* **1993**, *17*, 245. (b) Bollinger, M.; Vannice, M. A. *Appl. Catal. B: Environmental* **1996**, *8*, 417.
- (7) Valden, M.; Lai, X.; Goodman, D. W. *Science* **1998**, *281*, 1647.
- (8) Jia, J.; Haraki, K.; Kondo, J. N.; Domen, K.; Tamaru, K. *J. Phys. Chem. B* **2000**, *104*, 11153.
- (9) (a) Zhang, L.; Persaud, R.; Madey, T. E. *Phys. Rev. B* **1997**, *56*, 10549. (b) Cosandey, F.; Zhang, L.; Madey, T. E. *Surf. Sci.* **2001**, *474*, 1.
- (10) Rodriguez, J. A.; Chaturvedi, S.; Kuhn, M.; van Ek, J.; Diebold, U.; Robbert, P. S.; Geisler, H.; Ventrice, C. A. *J. Chem. Phys.* **1997**, *107*, 9146.

- (11) (a) Bondzie, V. A.; Parker, S. C.; Campbell, C. T. *J. Vac. Sci. Technol. A* **1999**, *17*, 1717. (b) Bondzie, V. A.; Parker, S. C.; Campbell, C. T. *Catal. Lett.* **1999**, *63*, 143. (c) Ajo, H. M.; Bondzie, V. A.; Campbell, C. T. *Catal. Lett.* **2002**, *78*, in press.
- (12) Yang, Z.; Wu, R.; Goodman, D. W. *Phys. Rev. B* **2000**, *61*, 14066.
- (13) Parker, S. C.; Grant, A. W.; Bondzie, V. A.; Campbell, C. T. *Surf. Sci.* **1999**, *441*, 10.
- (14) (a) Okumura, M.; Nakamura, S.; Tsubota, T.; Nakamura, T.; Azuma, M.; Haruta, M. *Catal. Lett.* **1998**, *51*, 53. (b) Hayashi, T.; Tanaka, K.; Haruta, M. **1998**, *178*, 566.
- (15) (a) Campbell, C. T. *Curr. Opin. Solid State Mater. Sci.* **1998**, *3*, 439. (b) Cosandey, F.; Madey, T. E. *Surf. Rev. Lett.* **2000**, *8*, 8. (c) Rainer, D. R.; Xu, C.; Goodman, D. W. *J. Mol. Catal. A: Chem.* **1997**, *119*, 307.
- (16) Lopez, N.; Nørskov, J. To be submitted for publication.
- (17) Cunningham, D. A. H.; Vogel, W.; Kageyama, H.; Tsubota, S.; Haruta, M. *J. Catal.* **1998**, *177*, 1.
- (18) Sanchez, A.; Abbet, S.; Heiz, U.; Schneider, W. D.; Hakkinen, H.; Barnett, R. N.; Landman, U. *J. Phys. Chem. A* **1999**, *103*, 9573.
- (19) Wallace, W. T.; Whetten, R. L. *J. Phys. Chem. B* **2000**, *104*, 10964.
- (20) Barteau, M. A. *Chem. Rev.* **1996**, *96*, 1413.

Previous studies indicate that gold grows on TiO<sub>2</sub>(110) epitaxially forming two- or three-dimensional particles (Volmer–Weber growth mode).<sup>7,9,13</sup> The formation of two-dimensional clusters has been detected only at low gold coverages (<0.2 ML) and moderate temperatures (<350 K).<sup>7,13</sup> Even though thermodynamically the gold would prefer to form three-dimensional (3D) islands from the onset of growth, kinetic limitations constrain the growth initially to two-dimensional (2D) islands.<sup>13</sup> The critical gold coverage for a 2D→3D transition decreases with temperature, and increases with the defect density of the TiO<sub>2</sub> surface.<sup>7,13</sup> At elevated temperatures (~750 K) 3D particles are present on the oxide surface, without encapsulation of the Au islands by Ti suboxides.<sup>9a</sup> A direct link has been found between the size of the gold islands and their chemical activity.<sup>7</sup> Gold nanoparticles dispersed on TiO<sub>2</sub>(110) are able to catalyze the CO + 0.5O<sub>2</sub> → CO<sub>2</sub> reaction at 300 K.<sup>7</sup> The supported gold particles bond O atoms much stronger than extended Au(110) or Au(111) surfaces.<sup>11</sup> In this article, we show that they have an extraordinary ability to adsorb and dissociate SO<sub>2</sub>.

The destruction of SO<sub>2</sub> (DeSOx) is a very important problem in environmental chemistry.<sup>21,22</sup> SO<sub>2</sub> is frequently formed during the combustion of fossil-derived fuels in factories, power plants, houses, and automobiles.<sup>21–23</sup> Every year the negative effects of acid rain (main product of the oxidation of SO<sub>2</sub> in the atmosphere) on the ecology and corrosion of monuments or buildings are tremendous.<sup>21,23</sup> Thus, new environmental regulations emphasize the need for more efficient technologies to destroy the SO<sub>2</sub> formed in combustion processes.<sup>22,24,25</sup> Titania is the most common catalyst used in the chemical industry and oil refineries for the removal of SO<sub>2</sub> through the Claus reaction: SO<sub>2</sub> + 2H<sub>2</sub>S → 2H<sub>2</sub>O + 3S<sub>solid</sub>.<sup>22</sup> Different approaches are being tested for improving the performance of titania in DeSOx operations.<sup>22,25</sup> The addition of gold to TiO<sub>2</sub> produces desulfurization catalysts with a *high efficiency* for the cleavage of S–O bonds. In this respect, the Au/TiO<sub>2</sub> system is much more chemically active than either pure titania or gold.

In the present study, we use synchrotron-based high-resolution photoemission and first-principles density-functional slab calculations to examine the interactions between gold and titania, and to study the chemistry of SO<sub>2</sub> on Au/TiO<sub>2</sub>(110) surfaces. The mechanism for the chemical activation of gold/titania is more complex than expected. It is found that Au adatoms modify the rate of exchange of O vacancies between the bulk and surface of titania, a phenomenon that enhances the overall chemical reactivity of the system. Electronically perturbed Au adatoms can dissociate SO<sub>2</sub> per se or assist in the dissociation of the molecule on the oxide surface.

## II. Experimental and Theoretical Methods

**II.1. Photoemission Experiments.** The photoemission experiments for the deposition of Au on TiO<sub>2</sub>(110) or the adsorption of SO<sub>2</sub> on Au(111) and Au/TiO<sub>2</sub>(110) surfaces were performed in a standard ultrahigh-vacuum chamber (base pressure ~ 6 × 10<sup>-10</sup> Torr) that is part of the U7A beamline of the National Synchrotron Light Source (NSLS) at Brookhaven National Laboratory.<sup>24f,26,27</sup> This ultrahigh-vacuum (UHV) chamber contains a hemispherical electron energy analyzer with multichannel detection, instrumentation for low-energy electron diffraction (LEED), a quadrupole mass spectrometer, and a dual anode Mg/Al Kα source. The S 2p, Au 4f, and valence spectra were taken using a photon energy of 380 or 260 eV, whereas a photon energy of 625 eV was used to collect the Ti 2p and O 1s data. The binding energy scale of the photoemission spectra was calibrated by the position of the Fermi edge.<sup>26</sup> The overall instrumental resolution in the photoemission experiments was ~0.35 eV. This resolution is much better than that obtained with conventional XPS in previous studies for the Au/TiO<sub>2</sub>(110) system<sup>7,9,13</sup> and, therefore, allows a more detailed study of changes in the position of the Au 4f and Ti 2p core levels upon deposition of gold. The high resolution of the photoemission experiments at the synchrotron is a powerful tool for studying the surface chemistry of SO<sub>2</sub> and detecting several related sulfur species.<sup>28,29</sup>

Mounting of the TiO<sub>2</sub>(110) sample in the UHV chamber was done following the procedure described in ref 26. In short, the oxide sample was sandwiched between Ta plates that were spot welded to two Ta heating legs of a manipulator capable of cooling to 80 K and heating to 1100 K.<sup>26,30</sup> The TiO<sub>2</sub>(110) crystal was cleaned by ion bombardment with 1 keV Ne<sup>+</sup> ions at room temperature, followed by annealing in UHV for 10 min at 970 K.<sup>26,31,32</sup> This sample treatment produced a (1 × 1) LEED pattern, and previous studies using scanning tunneling microscopy<sup>31</sup> and photoemission<sup>32</sup> have shown that the resulting surface has O vacancies with a density of ~7%. Gold was vapor-deposited on the TiO<sub>2</sub>(110) surface at 300 K. The Au doser consisted of a resistive heated W basket with a drop of ultrapure Au inside.<sup>33</sup> The coverages of gold on the oxide surface were estimated by taking the ratio of intensities for the Au 4f<sub>7/2</sub> and Ti 2p<sub>3/2</sub> signals in XPS (Al Kα radiation) and photoemission and comparing it to values reported in the literature for the Au/TiO<sub>2</sub>(110) system (Figure 3 in ref 13). The values reported are only an approximation to the actual gold coverages, but we did verify that the Au/TiO<sub>2</sub>(110) systems under study here contained coverages well under a monolayer by comparing to the corresponding Au 4f<sub>7/2</sub> intensity for surfaces of pure metallic Au.<sup>33,34</sup> In a set of experiments we investigated the behavior of SO<sub>2</sub> on Au(111) or polycrystalline films of Au grown on Mo(110). The Au(111) and Mo(110) substrates were cleaned and mounted as described in refs 33 and 34.

SO<sub>2</sub> was dosed to TiO<sub>2</sub>(110), Au/TiO<sub>2</sub>(110), polycrystalline Au, and Au(111) surfaces through a glass-capillary array doser<sup>28</sup> positioned to face the sample at a distance of ~2 mm. The SO<sub>2</sub> exposures are based

- (21) Slack, A. V.; Holliden, G. A. *Sulfur Dioxide Removal from Waste Gases*, 2nd ed; Noyes Data Corporation: Park Ridge, NJ, 1975.
- (22) (a) Pieplu, A.; Saur, O.; Lavalley, J.-C.; Legendre, O.; Nedez, C. *Catal. Rev.-Sci. Eng.* **1998**, *40*, 409. (b) Evans, J.; Lee, H. In *Topics in Environmental Catalysis*; Rao, S. V., Ed.; Interscience: New York, 2001; pp 187–214.
- (23) Stern, A. C.; Boubel, R. W.; Turner, D. B.; Fox, D. L. *Fundamentals of Air Pollution*, 2nd ed; Academic: Orlando, FL, 1984.
- (24) (a) *Environmental Catalysis*; Armor, J. N., Ed.; ACS Symp. Ser. No. 552; American Chemical Society: Washington, DC, 1994. (b) Rodriguez, J. A. *Ciencia* **2001**, *9*, 139. (c) Shelef, M.; McCabe, R. W. *Catal. Today* **2000**, *62*, 35. (d) Paik, S. C.; Chung, J. S. *Appl. Catal. B* **1995**, *5*, 233. (e) Zhu, T.; Kundakovic, L.; Dreher, A.; Flytzani-Stephanopoulos, M. *Catal. Today* **1999**, *50*, 381. (f) Rodriguez, J. A.; Jirsak, T.; Gonzalez, L.; Evans, J.; Perez, M.; Maiti, A. *J. Chem. Phys.* **2001**, *115*, 10914. (g) Kauffmann, T. G.; Kaldor, A.; Stuntz, G. F.; Kerby, M. C.; Ansell, L. L. *Catal. Today* **2000**, *62*, 77.
- (25) Evans, J.; Lee, H.; Johnson, M.; Wu, Y.; Fisher, I. Private communication.

- (26) Rodriguez, J. A.; Hrbek, J.; Dvorak, J.; Jirsak, T.; Maiti, A. *Chem. Phys. Lett.* **2001**, *336*, 377.
- (27) Rodriguez, J. A.; Pérez, M.; Jirsak, T.; González, L.; Maiti, A.; Larese, J. *Z. J. Phys. Chem. B* **2001**, *105*, 5497.
- (28) (a) Rodriguez, J. A.; Jirsak, T.; Chaturvedi, S.; Hrbek, J. A. *J. Am. Chem. Soc.* **1998**, *120*, 11149. (b) Jirsak, T.; Rodriguez, J. A.; Hrbek, J. *Surf. Sci.* **1999**, *426*, 319. (c) Rodriguez, J. A.; Jirsak, T.; Chaturvedi, S.; Dvorak, J. *J. Mol. Catal. A: Chem.* **2001**, *167*, 47. (d) Rodriguez, J. A.; Jirsak, T.; Freitag, A.; Hanson, J. C.; Larese, J. C.; Chaturvedi, S. *Catal. Lett.* **1999**, *62*, 113.
- (29) Sun, Y.-M.; Sloan, D.; Alberas, D. J.; Kovar, M.; Sun, Z.-J.; White, J. M. *Surf. Sci.* **1994**, *319*, 34.
- (30) Rodriguez, J. A.; Jirsak, T.; Liu, G.; Hrbek, J.; Dvorak, J.; Maiti, A. *J. Am. Chem. Soc.* **2001**, *123*, 9597.
- (31) Hebenstreit, E. L. D.; Hebenstreit, W.; Diebold, U. *Surf. Sci.* **2000**, *461*, 87.
- (32) Hrbek, J.; Rodriguez, J. A.; Dvorak, J.; Jirsak, T. *Coll. Czech Chem. Commun.* **2001**, *66*, 1149.
- (33) Rodriguez, J. A.; Kuhn, M. *Surf. Sci.* **1995**, *330*, L657.
- (34) Rodriguez, J. A.; Dvorak, J.; Jirsak, T.; Hrbek, J. *Surf. Sci.* **2001**, *490*, 315.

on the ion gauge reading and were not corrected for the capillary array enhancement ( $>5$  enhancement factor with respect to background dosing).

**II.2. First-Principles Density Functional Calculations.** We carried out self-consistent first-principles calculations within the Kohn–Sham density–functional (DF) theory using a commercial version of the CASTEP code<sup>35</sup> available from Accelrys. CASTEP has an excellent track record in adsorption studies on  $\text{TiO}_2(110)$ <sup>26,30,36–39</sup> and other oxide surfaces.<sup>24f,27,35b,40–42</sup> In this code, the wave functions of valence electrons are expanded in a plane wave basis set with  $\mathbf{k}$ -vectors within a specified energy cutoff  $E_{\text{cut}}$ . Tightly bound core electrons are represented by nonlocal ultrasoft pseudopotentials.<sup>43</sup> Brillouin Zone integration is approximated by a sum over special  $k$ -points chosen using the Monkhorst–Pack scheme.<sup>44</sup> The exchange–correlation contribution to the total electronic energy is treated in a spin-polarized generalized-gradient corrected (GGA) extension of the local density approximation (LDA).<sup>45</sup> In all the calculations, the kinetic energy cutoff  $E_{\text{cut}}$  and the density of the Monkhorst–Pack  $k$ -point mesh were chosen high enough to ensure convergence of the computed structures and energetics. Since the DF calculations were performed at the GGA level, one can expect reasonable predictions for the bonding energies of the  $\text{SO}_2$  molecule on  $\text{TiO}_2(110)$  and  $\text{Au}/\text{TiO}_2(110)$ .<sup>46,47</sup> For the interaction of CO and NO with  $\text{TiO}_2(110)$ , DF-GGA calculations predict adsorption energies within an accuracy of 5 kcal/mol.<sup>30,36,46c</sup> An acceptable match is also found for the calculated and experimentally measured adsorption energies of S and  $\text{S}_2$  on  $\text{TiO}_2(110)$ .<sup>26,37</sup> In any case, in this work our main interest is in qualitative trends in the energetics, and not in absolute values. For each optimized structure, the partial charges on the atoms were estimated by projecting the occupied one-electron eigenstates onto a localized basis set with a subsequent Mulliken population analysis.<sup>48,49</sup> Mulliken charges have well-known limitations,<sup>50</sup> but experience has shown that they are nevertheless useful as a qualitative tool.

### III. Results and Discussion

**III.1. Reaction of  $\text{SO}_2$  with  $\text{Au}(111)$ ,  $\text{TiO}_2(110)$ , and  $\text{Au}/\text{TiO}_2(110)$ .** Figure 1 shows S 2p photoemission spectra for the adsorption of  $\text{SO}_2$  on  $\text{Au}(111)$  at 100 K and subsequent heating to higher temperatures. After dosing  $\sim 0.5$  L of  $\text{SO}_2$ , a physisorbed multilayer of the molecule (166–169 eV S 2p

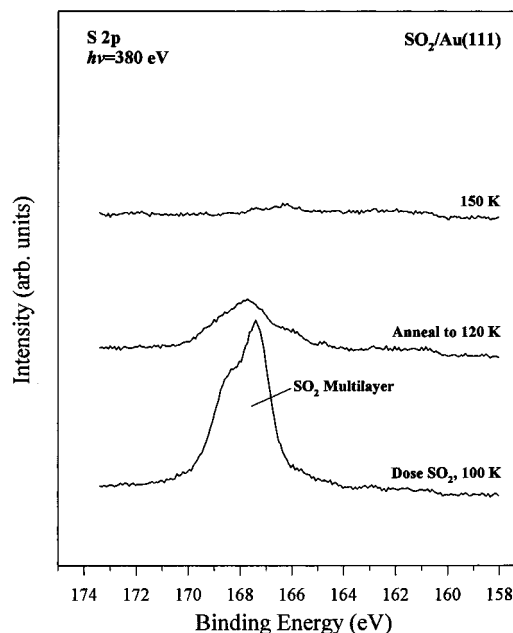


**Figure 1.** S 2p spectra acquired after depositing a multilayer of  $\text{SO}_2$  on  $\text{Au}(111)$  at 100 K, with subsequent heating to higher temperatures. The electrons were excited using a photon energy of 380 eV.

binding energy depending on film thickness and final-state relaxation<sup>28</sup>) is present on the metal surface at 100 K. Part of the physisorbed  $\text{SO}_2$  desorbs upon heating to 120 K and S 2p features appear at  $\sim 165.5$  eV due to chemisorbed  $\text{SO}_2$ .<sup>28</sup> By 150 K, most of the  $\text{SO}_2$  has disappeared from the gold surface and by 180 K nothing was left (not shown). In similar experiments for the adsorption of  $\text{SO}_2$  on a rough film ( $>20$  ML) of Au grown on a  $\text{Mo}(110)$  substrate, we again found desorption of the intact molecule at temperatures below 200 K. Thus, the adsorption bond of  $\text{SO}_2$  on bulk metallic gold is very weak (bonding energy  $<10$  kcal/mol) and the molecule does not dissociate. This can be contrasted with the behavior of  $\text{SO}_2$  on most transition metal surfaces,<sup>28a,28b,29,51,52</sup> where the molecule adsorbs strongly and readily decomposes at temperatures below 300 K. The only known exceptions to this trend are surfaces of silver, which adsorb the molecule reversibly,<sup>52–54</sup> but the  $\text{Ag}-\text{SO}_2$  bonds are still stronger than the  $\text{Au}-\text{SO}_2$  bonds. In the presence of  $\text{SO}_2$ , the surface of bulk gold behaves as an ideal “noble metal” with a negligible reactivity.

Figure 2 displays S 2p spectra taken after adsorbing  $\text{SO}_2$  on  $\text{TiO}_2(110)$  at room temperature. For small and large doses of  $\text{SO}_2$ , we found only a doublet in the S 2p region with the  $p_{3/2}$  component near 167.5 eV. This binding energy is consistent with the formation of a sulfate species on the oxide surface:<sup>28c,d</sup>



Previous photoemission<sup>55</sup> or XANES<sup>24f,56</sup> studies have reported

- (35) (a) Payne, M. C.; Allan, D. C.; Arias, T. A.; Johannopoulos, J. D. *Rev. Mod. Phys.* **1992**, *64*, 1045. (b) Milman, V.; Winkler, B.; White, J. A.; Pickard, C. J.; Payne, M. C.; Akhmatkaya, E. V.; Nobes, R. H. *Int. J. Quantum Chem.* **2000**, *77*, 895.
- (36) (a) Sorescu, D. C.; Rusu, C. N.; Yates, J. T. *J. Phys. Chem. B* **2000**, *104*, 4408. (b) Sorescu, D. C.; Yates, J. T. *J. Phys. Chem. B* **1998**, *102*, 4556. (c) Casarin, M.; Maccato, C.; Vittadini, A. *J. Phys. Chem. B* **1998**, *102*, 10752.
- (37) Rodriguez, J. A.; Hrbek, J.; Chang, Z.; Dvorak, J.; Jirsak, T.; Maiti, A. *Phys. Rev. B* **2002**, *65*, in press.
- (38) Dawson, I.; Bristowe, P. D.; Lee, M. H.; Payne, M. C.; Segall, M. D.; White, J. *Phys. Rev. B* **1996**, *54*, 13727.
- (39) Lindan, P. J. D.; Harrison, N. M.; Holender, J. M.; Gillan, M. J. *Chem. Phys. Lett.* **1996**, *261*, 246.
- (40) Rodriguez, J. A.; Maiti, A. *J. Phys. Chem. B* **2000**, *104*, 3630.
- (41) Refson, K.; Wogelius, R. A.; Fraser, D. G.; Payne, M. C.; Lee, M. H.; Milman, V. *Phys. Rev. B* **1995**, *52*, 10823.
- (42) (a) Rodriguez, J. A.; Jirsak, T.; Pérez, M.; Chaturvedi, S.; Kuhn, M.; González, L.; Maiti, A. *J. Am. Chem. Soc.* **2000**, *122*, 12362. (b) Rodriguez, J. A.; Pérez, M.; Jirsak, T.; González, L.; Maiti, A. *Surf. Sci.* **2001**, *477*, L279.
- (43) Vanderbilt, D. *Phys. Rev. B* **1990**, *41*, 7892.
- (44) Monkhorst, H. J.; Pack, J. D. *Phys. Rev. B* **1976**, *13*, 5188.
- (45) White, J. A.; Bird, D. M. *Phys. Rev. B* **1994**, *50*, 4954.
- (46) (a) Ziegler, T. *Chem. Rev.* **1991**, *91*, 651. (b) van Santen, R. A.; Neurock, M. *Catal. Rev.-Sci. Eng.* **1995**, *37*, 557. (c) Rodriguez, J. A. *Theor. Chem. Acc.* **2002**, *107*, 117.
- (47) Rodriguez, J. A.; Jirsak, T.; Pérez, M.; González, L.; Maiti, A. *J. Chem. Phys.* **2001**, *114*, 4186.
- (48) Segall, M. D.; Pickard, C. J.; Shah, R.; Payne, M. C. *Phys. Rev. B* **1996**, *54*, 16317.
- (49) Segall, M. D.; Pickard, C. J.; Shah, R.; Payne, M. C. *Mol. Phys.* **1996**, *89*, 571.
- (50) (a) Szabo, A.; Ostlund, N. S. *Modern Quantum Chemistry*; McGraw-Hill: New York, 1989. (b) Wiberg, K. B.; Rablen, P. R. *J. Comput. Chem.* **1993**, *14*, 1504.

- (51) Rodriguez, J. A.; Ricart, J. M.; Clotet, A.; Illas, F. *J. Chem. Phys.* **2001**, *115*, 454.

- (52) Haase, J. *J. Phys.: Condens. Matter* **1997**, *9*, 3647.
- (53) (a) Solomon, J. L.; Madix, R. J.; Wurth, W.; Stöhr, J. *J. Phys. Chem.* **1991**, *95*, 3687. (b) Rodriguez, J. A. *Surf. Sci.* **1990**, *226*, 101.
- (54) (a) Sun, Z.-J.; Gravelle, S.; Mackay, R. S.; Zhu, X.-Y.; White, J. M. *J. Chem. Phys.* **2001**, *99*, 10021. (b) Castro, M. E.; White, J. M. *J. Chem. Phys.* **1991**, *95*, 6057.
- (55) Sayago, D. I.; Serrano, P.; Bohme, O.; Goldoni, A.; Paolucci, G.; Roman, E.; Martín-Gago, J. A. *Phys. Rev. B* **2001**, *64*, 205402.

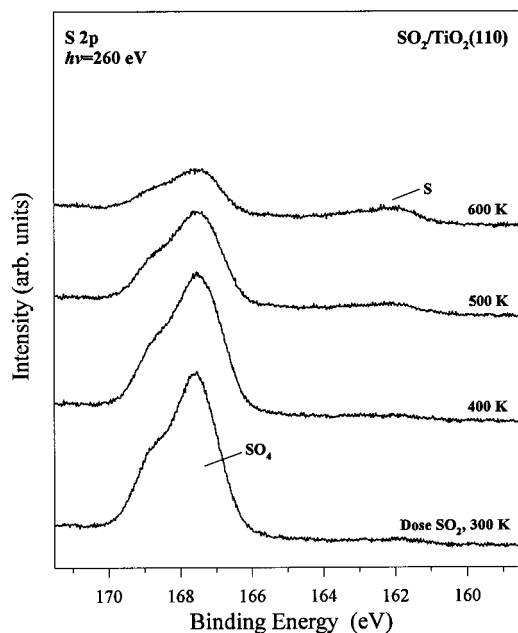


**Figure 2.** S 2p spectra taken after a  $\text{SO}_2$  saturation dose of 20 L to  $\text{TiO}_2$ (110) at 300 K, with subsequent heating to higher temperatures (400, 500, and 600 K). A photon energy of 260 eV was used to take these spectra.

an identical result for the adsorption of  $\text{SO}_2$  on  $\text{TiO}_2$ (110) and bulk powders of titania. At 300 K, decomposition of  $\text{SO}_2$  has been observed only on surfaces that are rich in O vacancies ( $\text{TiO}_{2-x}$ ).<sup>24f,56</sup> As seen in Figure 2 and the results in ref 55, heating to elevated temperatures induces the decomposition of the adsorbed sulfate and only a minor amount ( $<0.05$  ML) of atomic sulfur is deposited on the oxide surface (i.e. mainly  $\text{SO}_{4,\text{surface}} \rightarrow \text{SO}_{2,\text{gas}} + 2\text{O}_{\text{oxide}}$ ). Clearly, one has to find ways to promote the full decomposition of  $\text{SO}_2$  (or  $\text{SO}_x$  species in general) on titania.

Figure 3 shows S 2p spectra for the adsorption of  $\text{SO}_2$  on  $\text{Au}/\text{TiO}_2$ (110) surfaces at 300 K. The spectra in the top panel were taken after dosing  $\text{SO}_2$  directly after the deposition of Au on the oxide substrate at 300 K. For the spectra in the bottom panel, the  $\text{Au}/\text{TiO}_2$ (110) surfaces were prepared by dosing Au at 300 K, followed by brief annealing to 750 K, and in the final step  $\text{SO}_2$  was dosed at 300 K. Annealing at temperatures near 750 K is a step in the preparation of many  $\text{Au}/\text{TiO}_2$ (110) surfaces,<sup>7,9</sup> and these elevated temperatures are also used in DeSOx operations that use titania as a catalyst/sorbent.<sup>21,22,25</sup> It is known that Au wets poorly the  $\text{TiO}_2$ (110) substrate.<sup>7,9,13</sup> For the Au coverages in Figure 3, Au is expected to form 2D or 3D particles with an average diameter smaller than 10 nm.<sup>7</sup> For example, images of scanning tunneling microscopy (STM) for a  $\text{Au}/\text{TiO}_2$ (110) surface with 0.25 ML of gold (prepared in a way similar to that used to prepare the surfaces in the bottom panel of Figure 3 before dosing  $\text{SO}_2$ ) show clusters of the admetal with an average size of  $\sim 2.6$  nm in diameter and  $\sim 0.7$  nm in height (two or three atomic layers) located preferentially on the step edges of the  $\text{TiO}_2$ (110) substrate.<sup>7</sup> In the case of the surface with 0.05 ML of Au in Figure 3, Au should form 2D islands with an average diameter below 2.5 nm.<sup>7,13</sup>

The S 2p spectra in Figure 3 indicate that upon adsorption of  $\text{SO}_2$  on  $\text{Au}/\text{TiO}_2$ (110),  $\text{SO}_4$  and atomic S<sup>26,28c,34</sup> (produced

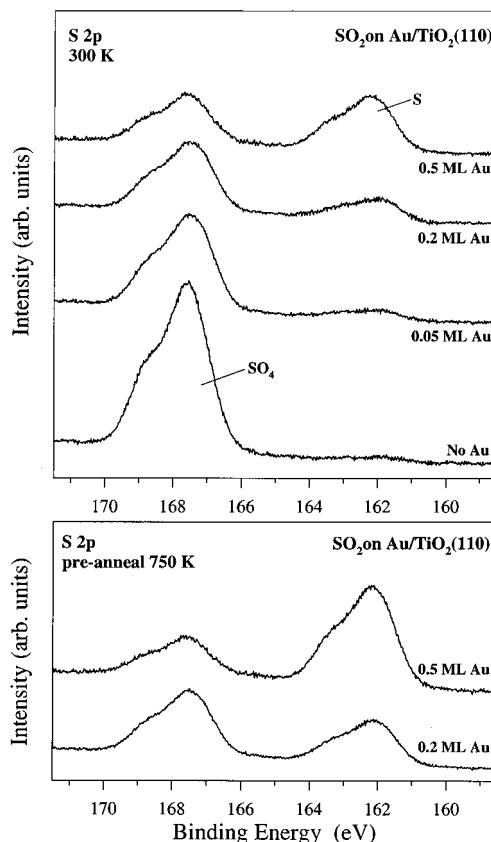


**Figure 3.** S 2p spectra for the adsorption of  $\text{SO}_2$  on  $\text{Au}/\text{TiO}_2$ (110) at 300 K. The spectra in the top panel are for  $\text{Au}/\text{TiO}_2$ (110) surfaces in which  $\text{SO}_2$  was dosed after depositing Au on  $\text{TiO}_2$ (110) at 300 K. On the other hand, the  $\text{Au}/\text{TiO}_2$ (110) surfaces in the bottom panel were prepared by deposition of Au at 300 K, followed by annealing at 750 K before dosing  $\text{SO}_2$  at room temperature. In these experiments, all the surfaces were exposed to 20 L of  $\text{SO}_2$ . The data were obtained using a photon energy of 260 eV.

by the full dissociation of  $\text{SO}_2$ ) coexist on the surface. The larger the Au coverage on titania (0.05  $\rightarrow$  0.5 ML range), the bigger the amount of atomic S deposited. This trend points to a direct involvement of gold in the dissociation of  $\text{SO}_2$ . Additional evidence for this fact is provided by the Au 4f spectra in Figure 4. The adsorption of  $\text{SO}_2$  on the  $\text{Au}/\text{TiO}_2$ (110) surface at 300 K produces a substantial attenuation in the Au 4f signal and a shift toward lower binding energy (a trend not seen in the Ti 2p core levels), which both are consistent with a direct interaction of supported gold with the decomposition products of  $\text{SO}_2$ . By comparing the photoemission results in Figures 1 and 3, it is clear that *Au nanoparticles dispersed on titania have an extraordinary reactivity toward  $\text{SO}_2$* . Whereas the surface of bulk metallic gold does not react with  $\text{SO}_2$ , the supported Au nanoparticles adsorb and dissociate the molecule with an activity comparable to that of surfaces of Ru, Rh, Ni, Pd, and Pt.<sup>28a,28b,29,52,57</sup>

In our studies, the relative amount of S deposited on a  $\text{Au}/\text{TiO}_2$ (110) surface increased when the sample was preannealed to 750 K after depositing Au at 300 K and before dosing  $\text{SO}_2$  (for an example, see Figure 3 and compare results for the same Au coverage). This is probably a consequence of generating active sites with special morphological<sup>7,9</sup> or electronic properties (Figures 4 and 5). In the left panel of Figure 4, when a clean

(56) Warburton, D. R.; Pundie, D.; Muryn, C. A.; Prakaharan, K.; Wincott, P. L.; Thornton, G. *Surf. Sci.* **1992**, 269/270, 305.

(57) (a) Rodriguez, J. A.; Jirsak, T.; Chaturvedi, S. *J. Chem. Phys.* **1999**, 110, 3138. (b) Rodriguez, J. A.; Hrbek, J. *Acc. Chem. Res.* **1999**, 32, 719.

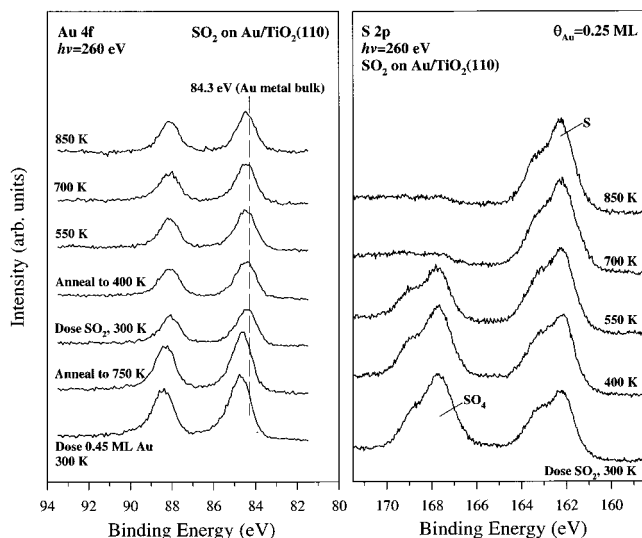


**Figure 4.** Left: Au 4f spectra for the reaction of SO<sub>2</sub> with a Au/TiO<sub>2</sub>(110) surface. Initially, 0.45 ML of Au was deposited on the oxide substrate at 300 K. Then, the Au/TiO<sub>2</sub>(110) system was heated to 750 K, and upon cooling to room temperature was exposed to 20 L of SO<sub>2</sub>. Subsequently, the temperature was increased from 300 to 850 K. The dashed line denotes the position measured in our instrument for bulk metallic gold. A photon energy of 260 eV was used to record the Au 4f spectra. Right: S 2p spectra for the adsorption of SO<sub>2</sub> on a Au/TiO<sub>2</sub>(110) surface at 300 K and subsequent annealing to elevated temperatures. Initially, 0.25 ML of Au was deposited on TiO<sub>2</sub>(110) at room temperature, and preannealed to 750 K before dosing with SO<sub>2</sub>. A photon energy of 260 eV was also used to record these data.

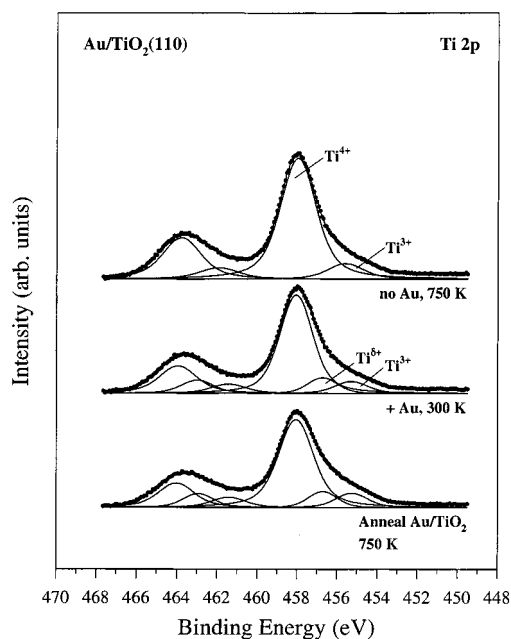


**Figure 5.** Ti 2p spectra taken before and after dosing 0.5 ML of gold to a TiO<sub>2</sub>(110) surface. In the first step, the clean oxide was annealed at 750 K, and then the top spectrum was recorded. This was followed by the dosing of Au at 300 K (middle) and final heating to 750 K (bottom). The spectra were obtained using a photon energy of 625 eV.

Au/TiO<sub>2</sub>(110) surface is heated from 300 to 750 K (bottom of the graph), there is a narrowing of the Au 4f peaks and a small shift ( $\sim 0.2$  eV) toward lower binding energy. The binding-energy shift could be interpreted as a minor increase in the electron density of the Au particles, if one assumes that it comes from initial state effects.<sup>58</sup> This interpretation is in agreement with the trends seen in Ti 2p photoemission spectra (Figure 5)

and the results of density functional calculations (section III.2). As we will see below, an increase in the electron density of gold favors interactions between the admetal and LUMO of SO<sub>2</sub>, facilitating the dissociation of the molecule. For the Au overlayers on TiO<sub>2</sub>(110), we measured Au 4f binding energies that were 0.4–0.6 eV larger than that found in our instrument for bulk metallic gold (dashed line in Figure 4). Similar shifts have been observed before in XPS studies,<sup>7,9a,12</sup> and are mainly a consequence of a large change in final state (i.e. a variation in the screening of the core-hole<sup>58</sup>) that overcomes changes in initial state that move the core levels of supported Au toward lower binding energy as shown by first-principles density-functional calculations.<sup>12</sup>

Figure 5 displays Ti 2p spectra collected before and after dosing Au to a TiO<sub>2</sub>(110) surface. At the photon energy used to take the spectra (625 eV), we were measuring only the composition of the first 2–3 layers of the sample.<sup>59</sup> The surface without gold (top) was initially annealed at 750 K for 2 min to induce the formation of O vacancies.<sup>31,32</sup> In this way, one obtains a distribution of vacancies from the surface to the bulk of the sample.<sup>31,60,61</sup> The Ti 2p spectrum for this system is well fitted<sup>62</sup> by a set of two doublets with p<sub>3/2</sub> components at 458.03 (Ti<sup>4+</sup> <sup>32</sup>) and 455.96 eV (Ti<sup>3+</sup> <sup>32</sup>). Under these conditions, the near surface region contains O vacancies with a density of  $\sim 7\%$ .<sup>31,32</sup> When Au is deposited on this surface at 300 K, the features between 454 and 456 eV gain relative intensity with respect to the main feature at  $\sim 458$  eV and the resulting Ti 2p spectrum needs three doublets for a good fit (center of Figure 5). The p<sub>3/2</sub> components of these doublets appear at 458.06, 456.93, and 455.41 eV. The first peak is due to Ti<sup>4+</sup> cations, the last one corresponds to Ti<sup>3+</sup> species, and the middle one can be assigned to Ti<sup>3+</sup> ions weakly oxidized (Ti<sup>δ+</sup>) by interaction with Au. Final annealing of the Au/TiO<sub>2</sub>(110) surface at 750 K produces a clear increase in the intensity of the Ti<sup>3+</sup> and Ti<sup>δ+</sup> peaks. This phenomenon is not a consequence of the oxidation of Au,<sup>9a,63</sup> or the evolution of O<sub>2</sub> into the gas phase.<sup>64</sup> It originates in the migration of O vacancies from the bulk to the surface of the oxide. As we will see in section III.2, Au adatoms enhance the relative stability of surface vacancies. *One has a complex situation, in which the admetal modifies the rate of vacancy exchange between the bulk and surface of the oxide, and at the same time the presence of O vacancies in the surface perturbs electronically the gold making it more chemically active.*

The right panel in Figure 4 shows S 2p spectra taken after dosing SO<sub>2</sub> at 300 K to a Au/TiO<sub>2</sub>(110) surface with 0.25 ML of Au and preannealed to 750 K. The spectrum at the bottom is

(58) Egelhoff, W. F. *Surf. Sci. Rep.* **1987**, *6*, 253.

(59) See pp 382–383 in ref 1b.

(60) Henrich, V. E.; Cox, P. A. *The Surface Science of Metal Oxides*; Cambridge University Press: Cambridge, UK, 1994.

(61) (a) Derry, D. J.; Lees, D. G.; Calvert J. M. *J. Phys. Chem. Solids* **1981**, *42*, 57. (b) Sasaki, J.; Peterson, N. L.; Hoshino, K. *J. Phys. Chem. Solids* **1985**, *46*, 1267.

(62) After subtracting a Shirley background from the raw data, the curves were fitted by a convolution of a Gaussian–Lorentzian sum and an asymmetric function.<sup>32</sup>

(63) (a) Since titania is much more stable than any oxide of gold,<sup>63b</sup> a TiO<sub>2</sub> + Au → TiO<sub>2-x</sub> + AuO<sub>x</sub> reaction is highly endothermic. (b) *Lange's Handbook of Chemistry*, 13th ed.; Dean, J. A., Ed.; McGraw-Hill: New York, 1985.

(64) In experiments similar to those in Figure 5, no evidence was found for the desorption of O<sub>2</sub> during the heating of Au/TiO<sub>2</sub>(110) surfaces from 300 to 750 K. In addition, density-functional calculations (ref 16 and section III.2) indicate that a substitution of the TiO<sub>2</sub> + Au → TiO<sub>2-x</sub>Au + O<sub>2,gas</sub> type is substantially endothermic and unlikely.

for a saturation dose of  $\text{SO}_2$  and shows strong features for  $\text{SO}_4$  and atomic S. At small doses of  $\text{SO}_2$  (not shown) only the doublet for atomic S was seen. When the temperature was raised from 300 to 700 K, the features for  $\text{SO}_4$  disappeared, due to desorption of  $\text{SO}_2$  and a  $\text{SO}_4 \rightarrow \text{S}$  transformation. The features for S adatoms were still present upon annealing to 1100 K. Identical results were found for other Au/ $\text{TiO}_2(110)$  surfaces. At 300 K the sticking coefficient of  $\text{SO}_2$  on the supported Au nanoparticles or the Au– $\text{TiO}_2$  interface was much bigger than that on the pure oxide support (sites for  $\text{SO}_4$  formation), and for dosing of  $\text{SO}_2$  at elevated temperatures ( $\geq 700$  K) only features for atomic S were observed in the S 2p spectra. Photoemission data for the Au 4f core levels indicated that in all cases the gold was interacting with the S deposited by the decomposition of  $\text{SO}_2$  (see Figure 4 for an example). The same can be expected for the O adatoms. Au particles on  $\text{TiO}_2(110)$  bond O atoms  $\sim 40\%$  more strongly than bulk Au.<sup>11</sup>

The results presented above suggest that the addition of Au nanoparticles should be an excellent route for facilitating the cleavage of S–O bonds on titania catalysts. The O adatoms deposited by the decomposition of  $\text{SO}_2$  can be removed by reaction with H or  $\text{CO}$ ,<sup>5,7</sup> while the S adatoms can form  $\text{S}_n$  aggregates at high temperatures.<sup>22</sup> Indeed, recent catalytic tests for the Claus reaction ( $\text{SO}_2 + 2\text{H}_2\text{S} \rightarrow 2\text{H}_2\text{O} + 3\text{S}_{\text{solid}}$ ) and the reduction of  $\text{SO}_2$  by carbon monoxide ( $\text{SO}_2 + 2\text{CO} \rightarrow 2\text{CO}_2 + \text{S}_{\text{solid}}$ ) show that the Au/ $\text{TiO}_2$  system is 5–10 times more active than pure  $\text{TiO}_2$ .<sup>25</sup> (Interestingly, polycrystalline foils of gold are inactive as catalysts for these DeSOx processes.<sup>22,25</sup>) In the next section, we will use density functional (DF) calculations to understand and explain the remarkable reactivity of Au/ $\text{TiO}_2(110)$  surfaces.

**III.2. Bonding of  $\text{SO}_2$  to  $\text{TiO}_2(110)$  and Au/ $\text{TiO}_2(110)$ .** In the first part of this section, we will study the coadsorption of  $\text{SO}_2$  and Au on an ideal or perfect  $\text{TiO}_2(110)$  surface. In the second part, the results of the DF calculations will show the important role played by O vacancies in the chemistry of the  $\text{SO}_2/\text{Au}/\text{TiO}_2(110)$  system, and how they affect and are affected by Au adatoms. The  $\text{TiO}_2(110)$  surface was represented by a four-layer slab as shown in Figure 6, which was embedded in a three-dimensionally periodic supercell.<sup>26,35</sup> A vacuum of 14 Å was placed on top of the slab to ensure negligible interactions between periodic images normal to the surface.<sup>35</sup> The adsorbates ( $\text{SO}_2$ , Au) were set only on one side of the slab, and their geometry and the geometry of the first two slab layers were relaxed during the DF calculations. This has proven to be a reliable model to study the adsorption of CO, NO,  $\text{NO}_2$ , and S on  $\text{TiO}_2(110)$ .<sup>26,30,37,46c</sup> The DF calculations predicted accurate lattice constants for bulk  $\text{TiO}_2$  and a structural geometry for the clean  $\text{TiO}_2(110)$  surface that was in agreement with several theoretical and experimental investigations.<sup>26,30</sup>

It is known that  $\text{SO}_2$  can bond to oxides via its S or O atoms.<sup>28,29,47,52,53</sup>  $\text{SO}_2$  was adsorbed ( $\theta_{\text{SO}_2} = 0.25$  ML) on a perfect  $\text{TiO}_2(110)$  surface through O bonded to two neighboring Ti atoms ( $\eta^2\text{-O}_2$ ), through S on a Ti atom ( $\eta^1\text{-S}$ ), or through S on one or two atoms in the bridging O rows ( $\eta^1\text{-S}$ ,  $\text{SO}_3^-$ , or  $\text{SO}_4$ -like species). All these configurations were found to be less stable than the hybrid conformation shown at the top of Figure 7 where  $\text{SO}_2$  interacts with an O and two Ti centers of the surface ( $\eta^3\text{-S}_2\text{O}_2$ ). This configuration constitutes a  $\text{SO}_3$ -like species and has been observed in DF slab calculations for

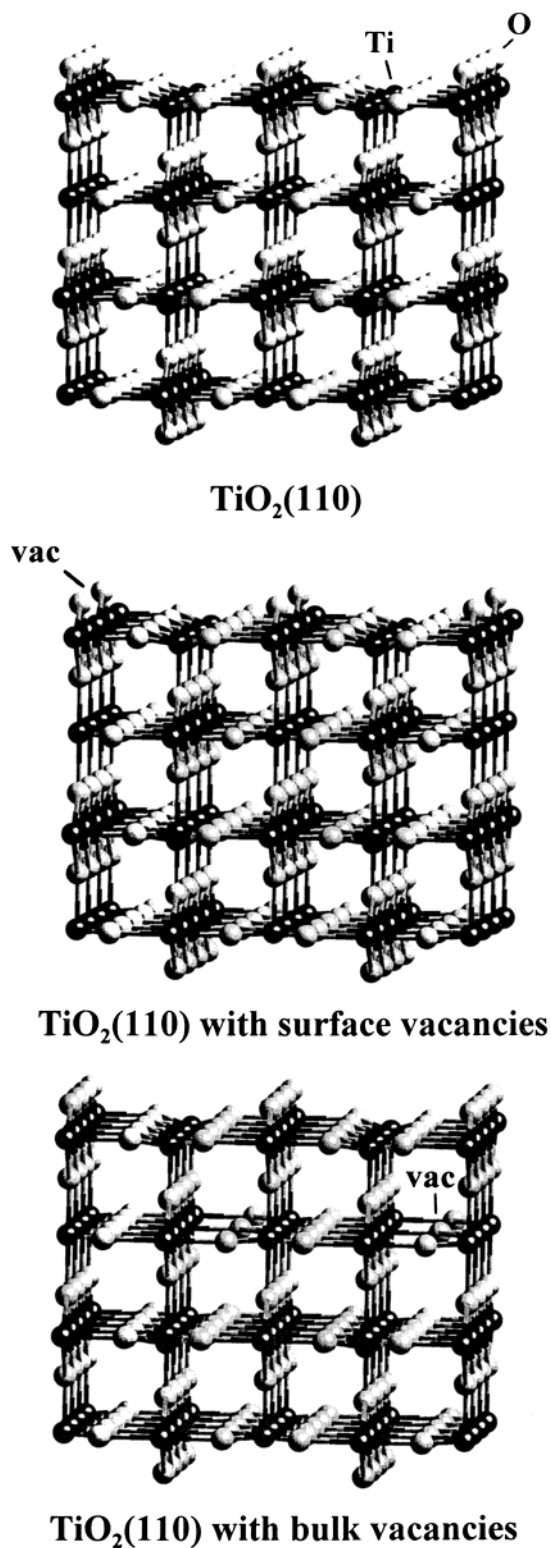


**Figure 6.** Slabs used to model a perfect  $\text{TiO}_2(110)$  surface, and systems with O vacancies in the surface (center) or subsurface (bottom) regions. Each slab contains four layers with Ti atoms. Ti atoms are represented by dark spheres, whereas gray spheres correspond to O atoms.

$\text{SO}_2$  on  $\text{MgO}(100)$ .<sup>65</sup> It has an adsorption energy of 15.1 kcal/mol. It may be the precursor for a  $\text{SO}_4$  species on a reconstructed

(65) (a) Rodriguez, J. A.; Jirsak, T.; Freitag, A.; Larese, J.; Maiti, A. *J. Phys. Chem. B* **2000**, *104*, 7439. (b) Schneider, W. F.; Li, J.; Hass, K. C. *J. Phys. Chem. B* **2001**, *105*, 6972.

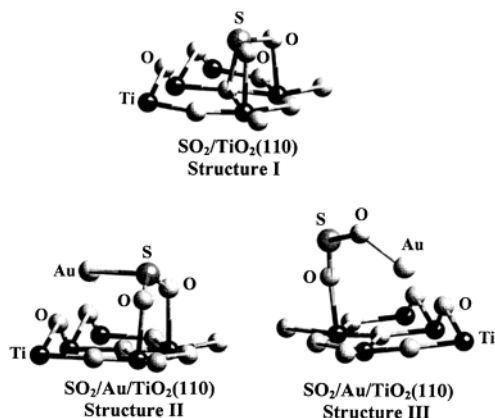


**Figure 7.** Most stable adsorption geometries for SO<sub>2</sub> on TiO<sub>2</sub>(110), structure I, and Au/TiO<sub>2</sub>(110), structures II and III. In structure I, the SO<sub>2</sub> molecule is attached to the surface in a  $\eta^3$ -S,O,O configuration with the oxygens bonded to two atoms in the Ti rows and the sulfur bonded to an in-plane O. In structure II, the Au is on a BO site bonded to two atoms in the bridging O rows and bonded to the sulfur in SO<sub>2</sub>. For structure III, the Au is on a HO site and bonded to an O atom of SO<sub>2</sub>.

TiO<sub>2</sub>(110) surface. On a perfect TiO<sub>2</sub>(110) surface, we found that the formation of SO<sub>4</sub> via direct adsorption of SO<sub>2</sub> on atoms of the bridging O rows or oxygens in the surface plane is not the most stable configuration. A similar fact has been observed in theoretical calculations for the adsorption of SO<sub>2</sub> on MgO(100),<sup>65,66</sup> where the formation of SO<sub>4</sub> requires reconstruction of the surface or interactions with defect sites.<sup>65b,66a</sup>

All-electron<sup>12</sup> and pseudopotential<sup>16</sup> DF calculations have been used to study the interaction of Au with slabs of TiO<sub>2</sub>(110). These calculations assume periodic arrays of Au atoms on the oxide surface. Such models neglect Au $\leftrightarrow$ Au interactions (i.e. no Au clusters or particles are included), but are useful for examining the effects of Au $\leftrightarrow$ TiO<sub>2</sub> interactions and the reactivity of the metal/oxide interface.<sup>12,16,67</sup> We followed the same approach to study the adsorption of SO<sub>2</sub> on a Au/TiO<sub>2</sub>(110) surface with a quarter of a monolayer of Au in a p(2 $\times$ 2) array. The Au atoms were positioned directly on top of Ti atoms (TTi), on the bridge between two Ti atoms (BTi), bonding two O atoms located in the bridging O rows (BO), or above the pseudo-hollow site formed by two in-plane O atoms and one O in the bridging O rows (HO). The HO site was 1.2 kcal/mol more stable than the TTi and BTi sites, which showed very similar stability. At 300 K and higher temperatures, Au adsorption on any of these sites is possible. These sites were 7–9 kcal/mol more stable than the BO site. A very similar trend has been found in all-electron DF calculations for a full layer of Au on TiO<sub>2</sub>(110).<sup>12</sup> After a Mulliken population analysis,<sup>48,49</sup> we found essentially covalent bonding between Au and TTi sites. A minor depletion of electrons (<0.1 e) on Au was observed when the element was bonded to O centers of the surface. The deposition of Au on TiO<sub>2</sub>(110) led to the appearance of occupied metal-induced states above the TiO<sub>2</sub> valence band (center of Figure 8), as seen in other DF slab calculations.<sup>12,16</sup>

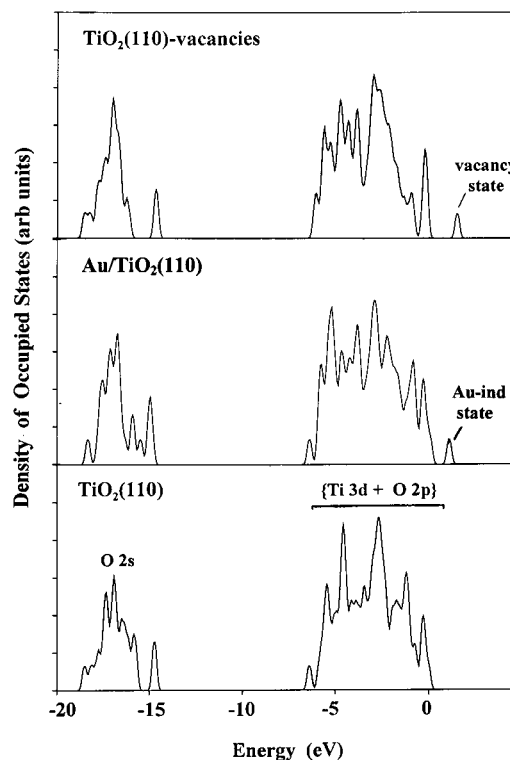


**Figure 8.** Density functional results for the density-of-states (DOS) of the occupied bands in TiO<sub>2</sub>(110), Au/TiO<sub>2</sub>(110), and a TiO<sub>2-x</sub>(110) system with O vacancies in the surface. The zero of energy in the figure is not the vacuum level.<sup>35</sup>

*The Au $\leftrightarrow$ TiO<sub>2</sub> interactions enhance the chemical activity of gold.* For the bonding of SO<sub>2</sub> to a single Au atom, the DF calculations predict a  $\eta^1$ -S conformation with a bonding energy of 6.9 kcal/mol. (A  $\eta^1$ -S conformation has been found for SO<sub>2</sub> on silver surfaces.<sup>53</sup>) When the Au atom is deposited on a HO site of the TiO<sub>2</sub>(110) surface, the bonding energy of the SO<sub>2</sub> to Au in a  $\eta^1$ -S conformation (without direct interaction of the molecule with TiO<sub>2</sub>) increased to 10.8 kcal/mol. The bottom of Figure 7 shows the two more stable adsorption geometries found for SO<sub>2</sub> on a p(2 $\times$ 2)-Au/TiO<sub>2</sub>(110) surface. They involve simultaneous bonding of SO<sub>2</sub> to Au and the oxide. (Similar interfacial adsorption sites have been found to be the most stable for propene on Au/TiO<sub>2</sub>(110).<sup>11c</sup>) Structure II is a modification of the geometry found for SO<sub>2</sub> on TiO<sub>2</sub>(110), structure I, with Au bonded to S and an SO<sub>2</sub> adsorption energy<sup>68</sup> of 24.2 kcal/mol. In structure III, SO<sub>2</sub> bonds via the oxygen atoms with an adsorption energy<sup>68</sup> of 21.3 kcal/mol. In structures II and III, there is a significant elongation of the S–O bonds (1.47–1.49 Å) with respect to the free molecule (1.43 Å) and structure I (1.44 Å). Thus, the presence of Au in the surface facilitates the dissociation of the SO<sub>2</sub> molecule.

Next, we will focus our attention on the effects of O vacancies on the chemistry of SO<sub>2</sub> on Au/TiO<sub>2</sub>(110). To model a TiO<sub>2</sub>(110) surface with O vacancies, we used a four-layer periodic slab with atoms missing from the bridging oxygen rows in the first layer (center of Figure 6).<sup>26,30,37</sup> In many situations it is unlikely that O vacancies in TiO<sub>2</sub> will assume a periodic array such as shown in Figure 6, but our model represents well the electronic and chemical perturbations associated with the

(66) (a) Pacchioni, G.; Clotet, A.; Ricart, J. M. *Surf. Sci.* **1994**, *315*, 337. (b) Pacchioni, G.; Ricart, J. M.; Illas, F. J. *Am. Chem. Soc.* **1994**, *116*, 10152.

(67) In DF-GGA calculations (Becke-88 for exchange and Perdew-91 for correlation) modeling the adsorption of SO<sub>2</sub> on a Au<sub>8</sub> particle<sup>18</sup> supported over a Ti<sub>7</sub>O<sub>9</sub> cluster embedded in an array of point charges,<sup>36c</sup> we found the strongest interactions of the adsorbate on Au atoms bonded to the oxide surface. The Au–TiO<sub>2</sub> interface was more chemically active than the “top” of the Au<sub>8</sub> particle. In a similar way, the most stable adsorption site for propene on Au/TiO<sub>2</sub>(110) involves simultaneous bonding to both gold and titania.<sup>11c</sup>

(68) The reference systems in this case are the individual SO<sub>2</sub> molecule and the p(2 $\times$ 2)-Au/TiO<sub>2</sub>(110) surface in its most stable conformation.

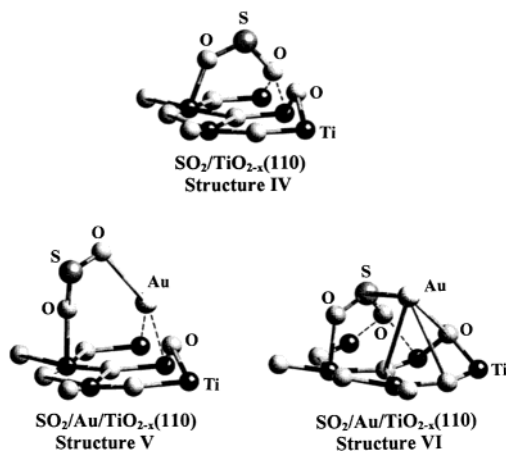


**Figure 9.** Most stable bonding conformations for SO<sub>2</sub> on TiO<sub>2-x</sub>(110), structure IV, and Au/TiO<sub>2-x</sub>(110), structures V and VI. The dashed lines denote interactions with O vacancy sites. In structure V, a Au atom is “capping” an O vacancy. In structure VI, the Au has moved to a HO site and the SO<sub>2</sub> is interacting directly with an O vacancy.

formation of O vacancies.<sup>26,30,37</sup> The top panel in Figure 8 displays the calculated density-of-states for the occupied bands in the TiO<sub>2-x</sub>(110) slab after full relaxation of the first two layers.<sup>30</sup> The introduction of O vacancies in the TiO<sub>2</sub>(110) surface generates a new occupied state that appears ~1.6 eV above the top of the valence band of titania. This state has been observed in experiments of valence photoemission,<sup>26,60</sup> and plays a dominant role in interactions with Au and SO<sub>2</sub>.

The top of Figure 9 shows the most stable geometry found for 0.25 ML of SO<sub>2</sub> on the TiO<sub>2-x</sub>(110) slab with surface vacancies, structure IV. One of the oxygens in SO<sub>2</sub> is directly above an O vacancy and the other is bonded to a Ti cation. The vacancy state in Figure 8 is in a good energy position for bonding interactions with the LUMO of SO<sub>2</sub>, and the result is a big adsorption energy (53.8 kcal/mol) with a large elongation in the S–O bonds (1.49–1.53 Å) due to a substantial oxide → SO<sub>2</sub> charge transfer (~0.5 e). This certainly favors the decomposition of the adsorbate, but an even better precursor state for dissociation is found when Au is coadsorbed with SO<sub>2</sub> on the oxide surface.

On oxygen vacancies the calculated energy of adsorption of Au atoms was ~48 kcal/mol larger than that on the most stable adsorption site (HO) of a perfect TiO<sub>2</sub>(110) surface. Au adatoms should interact preferentially with this kind of defect.<sup>12,16</sup> In agreement with other DF studies,<sup>16</sup> we found that the Au adatoms gain a low negative charge (ca. -0.15 e) on the TiO<sub>2-x</sub>(110) surface. This charge is small when compared to that found after depositing Au or other metals on O vacancies of MgO(100).<sup>18,69</sup> Charge density maps indicate that most of the electron density left after removal of an O atom from MgO(100) is located directly above the vacancy site.<sup>69b,70</sup> This is not the case for TiO<sub>2-x</sub>(110),<sup>71</sup> and the delocalization of charge limits the oxide → Au electron transfer on titania.<sup>72</sup> Nevertheless, the change in the electron density of Au when going from

TiO<sub>2</sub>(110) to TiO<sub>2-x</sub>(110) is important and affects the position of the Au 4f core levels (Figure 4) and reactivity of Au. The bottom of Figure 9 shows predicted geometries for adsorption of SO<sub>2</sub> on p(2×2)-Au/TiO<sub>2-x</sub>(110) surfaces. Structure V is probably the first step in the adsorption of the molecule, and eventually should transform into structure VI, which is 17.2 kcal/mol more stable. Structure VI has an SO<sub>2</sub> adsorption energy, 62.3 kcal/mol,<sup>73</sup> larger than that found on Au/TiO<sub>2</sub>(110), 24.2 kcal/mol, or TiO<sub>2-x</sub>(110), 53.8 kcal/mol. This is the best precursor for the dissociation of SO<sub>2</sub>. Comparing structures IV and VI, in the presence of Au one finds an increase in the adsorption energy of SO<sub>2</sub> (~8.4 kcal/mol) and in the length of the S–O bonds (0.08–0.11 Å). In the configuration of structure VI, Au and the oxide work in a cooperative way to dissociate the SO<sub>2</sub> molecule. The active sites are at the Au–TiO<sub>2</sub> interface.<sup>67</sup>

DF calculations indicate that Au can enhance the chemical activity of the oxide by modifying the rate of exchange of O vacancies between the bulk and surface. Using the two slab models shown at the center and bottom of Figure 6, we compared the stability of O vacancies in the surface and subsurface regions of TiO<sub>2</sub>(110). After structural relaxation of the top two layers in each slab, the DF calculations predicted a small difference in stability (~3 kcal/mol) that favored the structure with subsurface vacancies. A similar result is found in other DF studies.<sup>16</sup> Thus, at temperatures ≥300 K, bulk and surface vacancies should coexist in a titania sample and this is what is observed experimentally.<sup>31,60,61</sup> When Au is present on the surface, the migration of O vacancies from the subsurface region to the surface (see Figure 10) becomes a highly exothermic process (ΔE = -41.6 kcal/mol). This is a much better reaction pathway for the generation of surface defects (and the corresponding Ti<sup>δ+</sup> sites, δ < 4) than a substitution reaction of the TiO<sub>2</sub> + Au → AuTiO<sub>2-x</sub> + O<sub>2,gas</sub> type, which is endothermic.<sup>74,16</sup> For the Ti atoms bonded to Au at the bottom of Figure 10 (in principle, cations near “capped” O vacancies), a Mulliken population analysis gave positive charges substantially smaller than those seen for Ti atoms bonded to six O neighbors (Ti<sup>4+</sup>), a behavior consistent with the existence of Ti<sup>δ+</sup> or perturbed Ti<sup>3+</sup> species in the Ti 2p spectra for Au/TiO<sub>2-x</sub>(110) in Figure 5.

DF calculations indicate that Au adatoms not only affect the mobility of O vacancies in titania but also can assist in their formation via reduction with atomic hydrogen.<sup>74</sup> Near defects and on flat (110) terraces of titania, the 2H + TiO<sub>2</sub> → TiO<sub>2-x</sub> + H<sub>2</sub>O reaction is easier from an energetic viewpoint if Au atoms are present on the oxide surface and interact with the formed O vacancies.<sup>74</sup> This is important since H adatoms are intermediates in the Claus reaction (SO<sub>2</sub> + 2H<sub>2</sub>S → 2H<sub>2</sub>O + S<sub>solid</sub>).<sup>22</sup> Thus, two key phenomena are probably responsible for the remarkable DeSOx activity found for Au/TiO<sub>2</sub> in our photoemission studies and recent catalytic tests.<sup>25</sup> First, interactions with titania electronically perturb gold, making it more

(69) (a) To be submitted for publication. (b) Giordano, L.; Goniakowski, J.; Pacchioni, G. *Phys. Rev. B* **2001**, *64*, 075417. (c) Abbet, S.; Sanchez, A.; Heiz, U.; Schneider, W.-D.; Ferrari, A. M.; Pacchioni, G.; Röscher, N. *J. Am. Chem. Soc.* **2000**, *122*, 3453.

(70) Pacchioni, G.; Ferrari, A. M.; Ierano, G. *Faraday Discuss.* **1997**, *106*, 155.

(71) (a) Albaret, T.; Finocchi, F.; Noguera, C. *Faraday Discuss.* **1999**, *114*, 285. (b) Lindan, P. J. D.; Harrison, N. M.; Gillan, M. J.; White, J. A. *Phys. Rev. B* **1997**, *55*, 15919.

(72) In fact, for the adsorption of SO<sub>2</sub> on O vacancies of MgO(100) the charge on the adsorbate (~1.2 e)<sup>24f</sup> is also larger than on O vacancies of TiO<sub>2</sub>(110) (~0.5 e).

(73) The reference systems in this case are the individual SO<sub>2</sub> molecule and the p(2 × 2)-Au/TiO<sub>2-x</sub>(110) surface with Au in the SHO site. This conformation, although not the most stable for clean Au/TiO<sub>2-x</sub>(110), allows a direct comparison of adsorption energies on vacancy sites of TiO<sub>2-x</sub>(110) and Au/TiO<sub>2-x</sub>(110).

(74) Rodriguez, J. A.; Gonzalez, L.; Xu, Y.-T.; Maiti, A. To be submitted for publication.



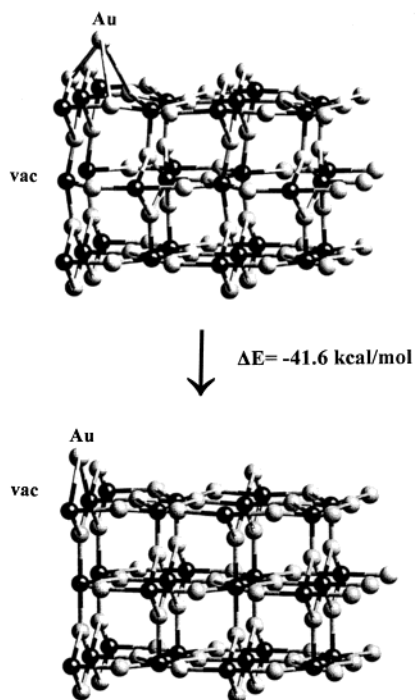


**Figure 10.** Gold induced migration of O vacancies. Initially, Au is adsorbed on a HO site of the surface and O vacancies are located in the subsurface or bulk region. In the final state, the O vacancies have moved to the surface and half of them are “capped” by gold atoms. In the scheme, only three of the four layers in the slab models are shown. Ti atoms are represented by dark spheres, whereas gray spheres correspond to O atoms.

chemically active. This effect is particularly significant when Au sits on O vacancies and the Au particles have a limited size (nanoscale range<sup>7,18</sup>). Second, gold enhances the chemical activity of titania by increasing the concentration of O vacancies at the surface of the oxide. The complex coupling of these two phenomena must be taken into consideration when trying to explain the high activity of Au/TiO<sub>2</sub> in other catalytic reactions.<sup>5–7,75</sup> Our experimental (Figure 5) and theoretical

results (Figure 10) show quite clearly that not only gold is perturbed when gold and titania interact. Thus, the oxide support can be more than a simple spectator in chemical transformations carried out on Au/TiO<sub>2</sub>.

#### IV. Conclusions

The deposition of Au nanoparticles on TiO<sub>2</sub>(110) produces a system with an extraordinary ability to adsorb and dissociate SO<sub>2</sub>. In this respect, Au/TiO<sub>2</sub> is much more chemically active than metallic gold or stoichiometric titania. On Au(111) and rough polycrystalline surfaces of gold, SO<sub>2</sub> bonds weakly (adsorption energy <10 kcal/mol) and desorbs intact at temperatures below 200 K. For the adsorption of SO<sub>2</sub> on TiO<sub>2</sub>(110) at 300 K, SO<sub>4</sub> is the only product (SO<sub>2</sub> + O<sub>oxide</sub> → SO<sub>4,ads</sub>). In contrast, Au/TiO<sub>2</sub>(110) surfaces ( $\theta_{\text{Au}} = 0.5$  ML) fully dissociate the SO<sub>2</sub> molecule under identical reaction conditions. The Au↔TiO<sub>2</sub> interactions are complex and simultaneously enhance the DeSOx activity of both gold and titania. Once Au bonds to titania, its ability to adsorb and dissociate SO<sub>2</sub> largely increases. In addition, Au adatoms modify the rate of exchange of O vacancies between the bulk and surface of titania, enhancing in this way the chemical activity of the oxide. The behavior of the SO<sub>2</sub>/Au/TiO<sub>2</sub>(110) system illustrates the importance of surface and subsurface O vacancies when dealing with the chemical properties of gold/titania.

**Acknowledgment.** The authors would like to thank J. Evans and H. Lee for discussions about the DeSOx properties of Au/TiO<sub>2</sub>, and N. Lopez for communication of DF results for Au/TiO<sub>2</sub>(110) before publication. This research was carried out at Brookhaven National Laboratory under contract DE-AC02-98CH10086 with the U.S. Department of Energy (Division of Chemical Sciences). The NSLS is supported by the Divisions of Materials and Chemical Sciences of DOE.

JA020115Y

(75) Kobayashi, T.; Haruta, M.; Tsubota, S.; Sano, H. *Sens. Actuators* **1990**, *B1*, 222.